DOI: 10.1002/anie.200806036

Nanostructures

One-Step Synthesis and Characterization of Gold–Hollow PbS_x Hybrid Nanoparticles**

Jian Yang,* JunJun Peng, Qingbo Zhang, Feng Peng, Hongjuan Wang, and Hao Yu

Inorganic hollow nanostructures with narrow size distribution and well-defined morphology have attracted extensive attention, as their unique structures and related physical properties are highly desirable in a number of applications.[1–7] For example, antibody-modified hollow gold nanostructures were demonstrated to be an excellent photothermal agent for cancer treatment, owing to their intense absorption in the near-infrared (NIR) region.[4] Carbon-coated hollow tin nanoparticles were employed as an anode material to improve the cycling performance of lithium batteries, as hollow structures can tolerate the large volume change in the electrodes during the course of charge and discharge.[5] Hollow palladium nanoparticles exhibited good catalytic ability in Suzuki cross-coupling reactions and could repeatedly be used without significant loss of catalytic activity.[6] Hollow platinum nanostructures showed superior electrocatalytic activity in oxidation of methanol, much better than their solid counterparts.[7] To date, a variety of synthetic strategies have been successfully developed to synthesize hollow nanostructures.[8–16] However, only few reports present hollow hybrid structures that are of several nanometers in size.[13,14]

Herein, syntheses of hollow hybrid nanostructures of PbS_x–Au of circa 10 nm are presented using a one-step reaction under mild experimental conditions. These hybrid nanoparticles are characterized by transmission electron microscope (TEM), selected area electron diffraction (SAED), energy dispersive X-ray spectroscopy (EDS), and X-ray photoelectron spectroscopy (XPS). The resultant hybrid nanostructures are built by solid gold and hollow PbS_x (nonstoichiometric lead sulfide) nanoparticles. Unlike the reported yolk–shell nanostructures,[13,14] synthesis of solid building units of gold on the surface of the PbS_x hollow structures are presented herein. Such hollow nanoparticles containing multiple components and well-defined structures on the order of 10 nm might have great application potential in many fields, such as heterogeneous catalysis, drug or gene delivery, and lithium batteries.

In brief, chloroauric acid ($HAuCl_4$) was dissolved in a toluene solution of tetraoctylammonium bromide (TOAB) and used as a gold precursor. Subsequently 0.3 mL of gold precursor was treated with 2 mL of 50 mM dodecylamine (DDA) at room temperature for several minutes. After the mixture was added dropwise into a 4 mL stock solution of PbS nanocrystals (Supporting Information, Figure S1) at elevated temperature, the product became totally different from initial PbS nanocrystals. Figure 1 presents typical TEM images, HRTEM images, and SAED pattern of the as-obtained product. Although the nanoparticles roughly preserve the same size as before, they show a relatively broad size distribution and a faceted shape. The former might be caused by the cooperation of the deposition reaction of gold and the etching reaction of PbS. The latter might be associated with various degrees of accessibility of the PbS nanocrystal surfaces owing to selective passivation of surfactants, and/or the higher reactivity at the regions with higher surface curvature and lower coordination number.[17,19–20] Further observation showed that the majority of the nano-

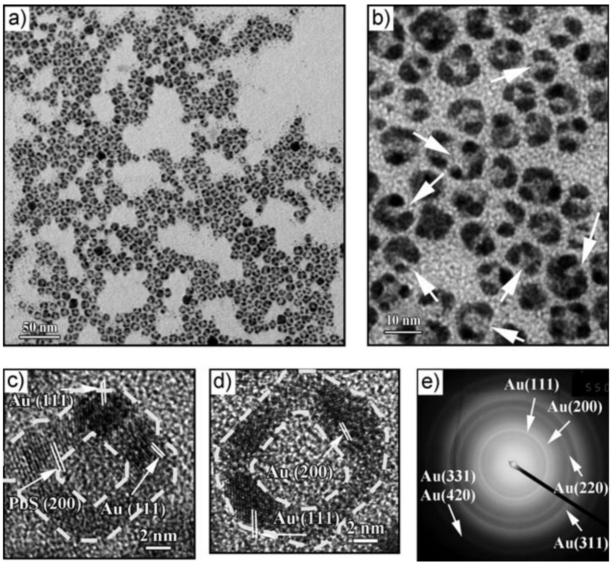

Figure 1. a,b) TEM images, c,d) HRTEM images, and e) SAED pattern of the hollow hybrid nanostructures. The reaction conditions are PbS (4 mL), dodecylamine (2 mL, 50 mM), gold precursor (0.3 mL comprising 20 mM $HAuCl_4$ and 50 mM TOAB), 80 °C, 1 h. The arrows in (b) indicate a typical structural feature of a pit, suggesting the voids are connected to the surface.

---

[*] Prof. J. Yang, J. Peng, Prof. F. Peng, Dr. H. Wang, Dr. H. Yu
Department of Chemical Engineering
South China University of Technology
Guangzhou 510640 (P.R. China)
E-mail: yangjian@scut.edu.cn
Dr. Q. B. Zhang
Department of Chemical Engineering
National University of Singapore
4 Engineering Drive 3, Singapore 117576 (Singapore)

[**] This work is supported in part by South China University of Technology (B10-D607009I1), Natural Science Foundation of China (no. 20801019) and Department of Education (no. 200805611041). PbS_x is nonstoichiometric lead sulfide.

Supporting information for this article is available on the WWW under http://dx.doi.org/10.1002/anie.200806036.

particles (> 70 %, Supporting Information, Figure S2) exhibited a significant contrast difference between the edge and the center, which was easily visible even under low magnification (Figure 1 a). As there are multiple chemical components in the product, the contrast differences arise possibly from a hollow structure or from a core–shell structure. To identify which one of these structures directly leads to the contrast difference, high-magnification and high-resolution TEM images were acquired.

The high-magnification TEM image of the nanostructures is shown in Figure 1 b. As a result of the strong imaging contrast, the dark dots on the surface could be assigned to elemental gold, which is also confirmed by the lattice fringes in the HRTEM images. It is found that each nanostructure is coated with gold nanoparticles that are 2–4 nm in size and these gold nanoparticles are randomly dispersed on the surface. The dispersion pattern of gold nanoparticles does not coincide with the contrast difference of the hybrid nanostructure in terms of shape and intensity. Thus, it is believed that the contrast difference in the hybrid nanostructure does not arise from gold nanoparticles deposited on the surface. Most importantly, many of the nanoparticles display the typical structure of a pit that is connected to the surface, as indicated by the arrows in Figure 1 b (Supporting Information, Figure S3). These openings on the surface that allows access to the hollow interior, exclude the possibility of a core–shell structure. Therefore, the as-obtained products can be identified as hollow hybrid nano-structures.

The crystallinity of the hollow hybrid nanoparticles was studied by HRTEM and SAED techniques. The gold nanoparticles on the nanostructure exhibit clear lattice fringes and random orientations, indicating crystalline nature and individual nucleation (Figure 1 c,d). Only a few walls present lattice fringes that could be indexed as the (200) crystal planes of PbS. The poor crystallinity of the wall is also supported by SAED pattern. In the SAED pattern only the diffraction rings of cubic-phase of gold are observed, further confirming that the hollow hybrid nanostructures are formed by solid crystalline gold particles on hollow structures containing amorphous walls (Figure 1 e).

The chemical components of the hollow hybrid nanostructures were studied by EDS and XPS techniques. Besides carbon, oxygen, and copper derived from surface-coated copper grids, EDS spectra also show the signals related to gold, lead, and sulfur (Supporting Information, Figure S4). As the strongest signals arising from gold, lead, and sulfur are quite close in the EDS spectra, the overlap of the signals make it difficult to obtain an unambiguous conclusion regarding the presence of these elements. Therefore, XPS spectra were obtained to further identify the elements and their chemical valences. The XPS spectra of the hollow hybrid nanostructures are summarized in Figure 2. The typical survey spectrum of the nanostructures is shown in Figure 2 a, confirming the presence of gold, lead, and sulfur. The high-resolution spectra of Au 4f, Pb 4f, and S 2p were also measured (Figure 2 b–d). The asymmetric nature of Au 4f (Figure 2 b) suggests multiple species of gold on the surface. The further deconvolution of the signals with Gaussian peaks reveals that there are two gold species in the nanostructures, gold(0) and gold(I).[21] The 4f5/2 and 4f7/2 peaks of gold(0) at 83.7 and 87.4 eV dominate the signal, which is consistent with the results from SAED and HRTEM. The weak 4f5/2 and 4f7/2 peaks of gold(I) centered around 85.3 and 88.9 eV might arise from the unreacted gold species adsorbed on the surface.[22] The high-resolution spectra of Pb 4f also show two species of lead on the surface. However, the two species are lead(II) in different chemical environments. The 4f5/2 and 4f7/2 peaks of lead(II) at 142.7 and 137.8 eV might originate from the sulfides.[21] The other set of 4f5/2 and 4f7/2 peaks of lead(II) at 143.7 and 138.9 eV derived from $PbCl_2$ might result either from the preparation of PbS nanocrystals or the reaction between the gold salt and PbS in the presence of DDA.[23] The broad peak of S 2p can be split into two peaks located at 162.8 and 161.7 eV, corresponding to S 2p1/2 and S 2p3/2 respectively. These values of the binding energies are much higher than the reported data of PbS (ca. 160.7 eV for S 2p3/2),[24] but close to those of disulfides and/or poly-sulfides (ca. 162.1 eV for S 2p3/2).[25] These values indicate that there might be some lead polysulfides in the product. The existence of polysulfides could also be justified by the reaction mechanism. These results indicate that sulfur in the product could be identified as nonstoichiometric lead sulfide (PbS_x). The transition from monosulfide to polysulfides would induce a mass of structural rearrangements and result in the poor crystallinity of the product, which is consistent with the amorphous nature of the wall. From the above results and the structural features, it is reasonable to believe that the hollow hybrid nanoparticles are composed of solid crystalline gold and hollow amorphous PbS_x.

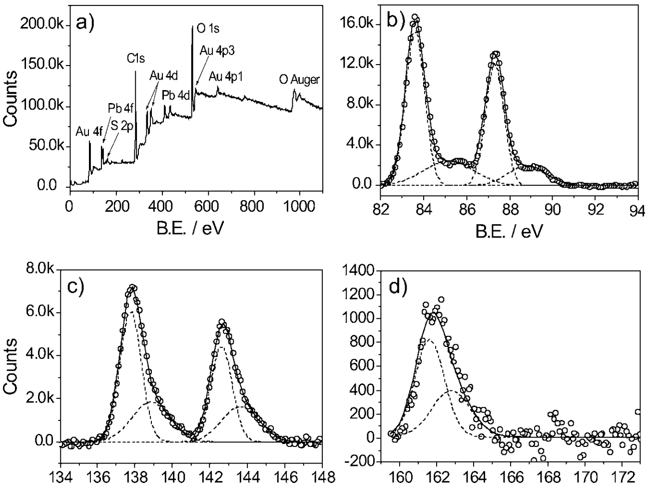

Figure 2. XPS spectra of the hollow hybrid nanostructures. a) The typical survey spectrum, b), c), and d) high-resolution spectra of Au 4f, Pb 4f, and S 2p. Deconvoluted peaks based on a Gaussian model (– – –) and their total contribution (——). k = 1000.

To understand the formation mechanism of the hollow hybrid nanostructures, the first question to address is the role of the reactants in the reaction. In other words, which reactant directly determines the formation of the hollow hybrid nanostructures? To address this question, we performed the following control experiments. Firstly, the reagents used in the synthesis were examined one by one at the same temperature and using the same reaction time. When DDA, TOAB, or both reacted with PbS nanocrystals, the product was still solid nanocrystals in a spherical shape. The results indicate that these reagents would not directly lead to the formation of hollow nanostructures, as presented in Figure 3 a–c. A large quantity of hollow hybrid nanostructures appeared in the product when the gold precursor was present in the reaction (Figure 3 d). This structural change, in other words, the formation of the hollow feature must be correlated with the gold salts in the gold precursor, as both DDA and TOAB could not produce such hollow structures. Secondly, this chemical etching of PbS nanocrystals induced by the gold salts is supported by another control experiment in which PbS nanocrystals were reacted with the gold precursor in the absence of DDA. The light-brown solution of PbS nanocrystals became colorless after the addition of the gold precursor (Supporting Information, Figure S5) and no product could be collected under high-speed centrifuge, suggesting a complete depletion of the PbS nanocrystals. As TOAB does not show such an effect on PbS nanocrystals, this experiment confirms again that the gold salts can effectively etch the PbS nanocrystals under appropriate conditions.

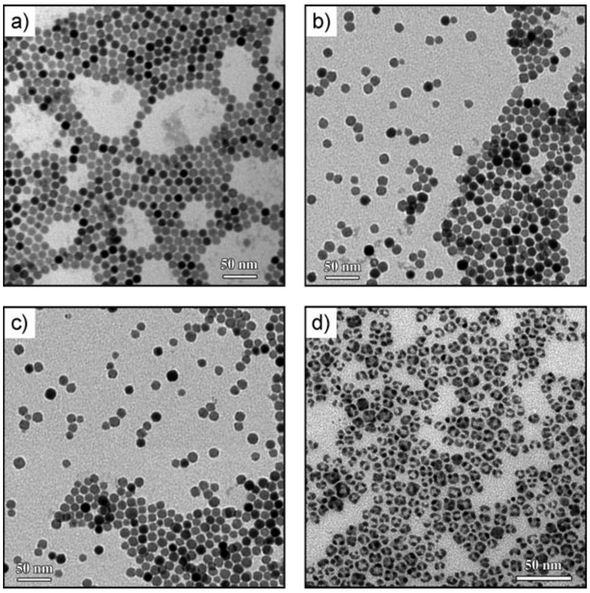

Figure 3. TEM images of the products obtained under different conditions. a) DDA, b) TOAB, c) DDA + TOAB, and d) DDA + gold precursor (TOAB and $HAuCl_4$). The reaction conditions are PbS (4 mL), 80 °C, and 1 h. Quantities used when applicable 50 mM DDA (2 mL), 50 mM TOAB (0.3 mL), and gold precursor (0.3 mL).

Figure 4 clearly presents the influence of the gold precursor on the product, as the amount of 50 mM DDA was kept at 2 mL. In the absence of the gold precursor, only spherical solid PbS nanocrystals were observed. If 0.1 mL of gold precursor was added into the solution of PbS nanocrystals at 80 °C, the deposition of gold led to the formation of dimeric nanostructures of PbS–Au (Figure 4 a), which is consistent with our previous report.[17] This result suggests that the deposition of gold possibly starts before the etching of PbS. As the amount of gold precursor was kept at 0.2 mL, the multiple nucleation of gold nanoparticles and the formation of small pits were observed in the product (Figure 4 b). As the amount of the gold precursor increased from 0.2 to 0.3 mL, a large quantity of hollow hybrid nanostructures were found in the product (Figure 4 c). Further increase of the gold precursor to 0.5 mL resulted in a large number of gold nanoparticles (Figure 4 d), indicating that most of the PbS nanocrystals were destroyed. These results not only confirm the chemical etching of the PbS nanocrystals using the gold precursors, but also offer an effective method to tune the voids in hollow hybrid nanostructures. It should be pointed out that there is an optimum concentration of the gold precursor for the formation of the hollow nanostructures. Otherwise, either solid nanoparticles or broken fragments are obtained in the product.

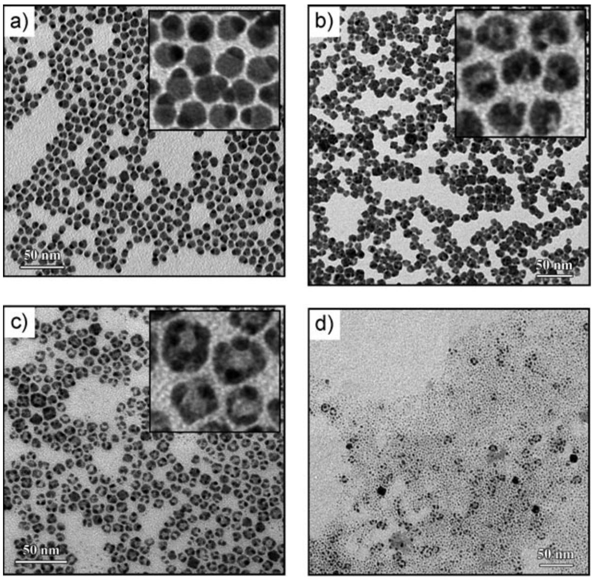

Figure 4. TEM images of the products obtained using different amounts of the gold precursor (20 mM HAuCl4 and 50 mM TOAB). a) 0.1 mL, b) 0.2 mL, c) 0.3 mL, and d) 0.5 mL. The other reaction conditions are PbS (4 mL), 50 mM DDA (2 mL), 80 °C, 1 h. The insets in (a–c) are the magnified TEM images of the corresponding products.

The second question to address would be to identify the particular reaction between the gold precursor and PbS that is responsible for the formation of hollow nanostructures. This question can be answered by comparing the amounts of lead and sulfur in the nanostructures before and after the reaction with the gold precursor. Elemental analysis based on inductively coupled plasma atomic emission spectroscopy (ICP-AES) shows that the amounts of lead and sulfur significantly decreased after addition of the gold precursor (Supporting Information, Table 1), indicating that both lead and sulfur participate in the reaction with the gold precursor. This fact excludes the possibility of a cation-exchange reaction between the reactants, but agrees with the redox reaction between $AuCl_4^-$ and sulfides.[25–28] In this redox reaction, there was a direct coupling of the reduction of gold salts and concomitant oxidation of sulfide, when gold-containing solutions was mixed with sulfide-based minerals. Meanwhile, lead ions were released into the solution and polysulfides were produced on the surface, which have been confirmed herein by XPS spectrum. The redox reactions between gold salts and chalcogenides have previously been reported not only for bulk materials,[25–28] but also for nanocrystal systems.[29]

As the redox reaction between the gold ions and the sulfides cause the dissolution of the PbS, the next question is why the redox reaction results in hollow hybrid nanostructures, and not just smaller particles. In other words, why is the redox reaction not isotropic at the surface? To answer this question, the role of DDA was taken into account. The influence of DDA on the products was studied with a volume of 0.3 mL of 20 mM $HAuCl_4$. At high concentration of DDA (250 mM), gold nanoparticles, both unattached and attached to solid PbS nanoparticles, were observed in the product (Supporting Information, Figure S6). The former can be attributed to the quick nucleation caused by the concentrated DDA solution. The latter can be assigned to the extremely good passivation of DDA on the surface of PbS so that $HAuCl_4$ does not have the opportunity to approach the surface of the PbS. This passivation effect leads to the disappearance of the hollow feature from the product. As the concentration of DDA decreased from 250 to 50 mM, the hollow feature was observed in the hybrid nanoparticles (Figure 3 d and 4 c). If the concentration was reduced further to 10 mM, no product could be obtained, indicating complete dissolution of PbS nanocrystals. These results clearly show that DDA not only effectively prohibits the etching of PbS induced by the gold salts but also makes the redox reaction between PbS and $HAuCl_4$ preferential at certain sites. Once the etching reaction takes place at a certain site of the surface, the as-produced pits roughen the local surface of nanoparticles exposing the surface that was previously protected by surfactants, and accelerate the etching toward the interior of the particle. Meanwhile, the surfactants on the neighboring surface of the pit effectively prohibit the etching reaction from propagating along the surface. The synergic cooperation of these two effects leads to an obvious hollow feature in the nanostructure. In this case, DDA plays a role similar to polyvinylpyrrolidon (PVP) in the preparation of palladium nanoboxes/nanocages and cetyltrimethylammonium bromide (CTAB) in the synthesis of CuO_x colloids.[30,31]

In fact, several different hybrid nanoparticles of PbS–Au have already been reported in the literature.[17,32,33] However, all these hybrid nanoparticles are built by solid building units. The result can be attributed to the different experiment conditions used in the preparation. For example, the heterodimer nanoparticles of PbS–Au reported by Zeng and coworkers were synthesized with gold nanoparticles as seeds to induce the formation of PbS nanocrystals.[32] But the PbS nanocrystals were pre-formed in our case and induce the formation of gold nanoparticles. The opposite synthetic order for PbS–Au presented herein results in different reactions mechanisms and gives rise to the differences in the structures of the products.

In summary, a one-step approach has been successfully developed for hollow hybrid PbS_x–Au nanoparticles, with a well-defined structure and narrow size distribution. These hybrid nanoparticles are built by hollow PbS_x nanoparticles and solid gold nanoparticles. The detailed control experiments show that the redox reaction of gold precursors with PbS nanocrystals in the presence of DDA leads to the hollow feature of hybrid nanostructures. The size of the voids in hollow hybrid nanostructures can be controlled, using different amounts of gold precursors. As similar redox reactions induced by gold salts take place not only on the surface of a number of bulk chalcogenides but also on their nanoscale counterparts, the approach described herein provides a reasonable and excellent way to produce hybrid nanostructures from hollow chalcogenides and solid gold nanoparticles. The hollow heterogeneous nanostructures not only offer a leap forward in the development of complex nanocrystal-based architectures, but also provide numerous opportunities for potential applications, such as drug delivery, DNA transferring, heterogeneous catalysis, and lithium-ion batteries.

Experimental Section

Lead chloride (99.0%), sulfur (99.0%), toluene (99.5%), ethanol (99.7%), and tetraoctylammonium bromide (99.0%) were purchased from Guanghua Chemical Factory Co. Ltd in Guangzhou and used without any further purification. Analytical grade $HAuCl_4{\cdot}x\,H_2O$ ($x=3$–5, Au $\approx$ 47.8%) was obtained from July Chemical Co. Ltd in Shanghai. Technical grade oleylamine ($\geq$ 70%) and dodecylamine (98%) were ordered from Fluka and Acros, respectively.

Preparation of PbS nanocrystals and gold precursor: the detailed preparation procedure for PbS nanocrystals follows those reported in literatures.[17,18] After the purification, PbS nanocrystals were dispersed in toluene with the concentration at 0.28 mM, which was used as the stock solution for later reaction. TOAB (0.546 g) was first dissolved in toluene (20 mL) to obtain the solution of TOAB (50 mM). Subsequently, an appropriate amount of $HAuCl_4{\cdot}x\,H_2O$ ($x=3$–5) was weighed and was dissolved in the above solution so that the concentrations of $HAuCl_4$ and TOAB in the final solution were kept as 20 and 50 mM, respectively. The toluene solution containing TOAB and $HAuCl_4$ was used as a gold precursor for the later reaction.

Preparation of hollow hybrid nanostructures of PbS–Au: In a typical procedure, an aliquot of the gold precursor (0.3 mL) was mixed with 50 mM dodecylamine (2 mL). The resulting solution was vortexed and allowed to stand for several minutes. The color of the solution changed from dark orange to light yellow, indicating the partial reduction of gold(III) in the solution. Stock solution of PbS nanocrystals (4 mL) was poured into a clean three-necked flask. The flask was then sealed by rubber septums, vacuumed, and purged with N_2 for 15 mins. The solution was heated to 80°C under vigorous stirring. After 15 mins, the light-yellow solution containing the gold precursor and dodecylamine was injected slowly. The solution was kept at that temperature for 1 h and then cooled down to room temperature. The clear solution was mixed with ethanol to precipitate the hybrid nanostructures. After centrifuging the solution, the precipitate was redispersed in toluene for TEM images.

TEM images were taken on an analytical transmission electron microscope of FEI Tecnai 12 with an acceleration voltage of 100 kV. The high-resolution TEM (HRTEM) images, SAED pattern, and EDS were obtained using trans-mission electron microscope (JEOL AEM 2010). XPS was performed on a photoelectron spectrometer (VG Scientific, ESCALAB MKII), using $Al_{K\alpha}$ radiation as an excitation source. Spectral correction was made using C 1s binding energy at 284.5 eV. ICP-AES were measured on a TJA IRIS(HR) spectrometer.

Received: December 11, 2008

Keywords: chalcogenides · corrosion · hybrid materials · nanocrystals

[1] a) H. C. Zeng, *J. Mater. Chem.* **2006**, *16*, 649–662; b) H. J. Fan, U. Gösele, M. Zacharias, *Small* **2007**, *3*, 1660–1671; c) X. W. Lou, L. A. Archer, Z. Yang, *Adv. Mater.* **2008**, *20*, 3987–4019.

[2] a) J. Shin, R. M. Anisur, M. K. Ko, G. H. Im, J. H. Lee, I. S. Lee, *Angew. Chem.* **2009**, *121*, 327–330; *Angew. Chem. Int. Ed.* **2009**, *48*, 321–324; b) H. P. Cong, S. H. Yu, *Adv. Funct. Mater.* **2007**, *17*, 1814–1820; c) J. Yang, Y. C. Liu, H. M. Lin, C. C. Chen, *Adv. Mater.* **2004**, *16*, 713–716.

[3] a) X. W. Lou, Y. Wang, C. Yuan, J. Y. Lee, L. A. Archer, *Adv. Mater.* **2006**, *18*, 2325–2329; b) Y. Wang, F. B. Su, J. Y. Lee, X. S. Zhao, *Chem. Mater.* **2006**, *18*, 1347–1353.

[4] J. Chen, D. Wang, J. Xi, L. Au, A. Siekkinen, A. Warsen, Z. Y. Li, H. Zhang, Y. Xia, X. Li, *Nano. Lett.* **2007**, *7*, 1318–1322.

[5] G. Cui, Y. Hu, L. Zhi, D. Wu, I. Lieberwirth, K. Mullen, *Small*, **2007**, *3*, 2066–2069.

[6] S. W. Kim, M. Kim, W. Y. Lee, T. Hyeon, *J. Am. Chem. Soc.* **2002**, *124*, 7642–7643.

[7] H. P. Liang, H. M. Zhang, J. S. Hu, Y. G. Guo, L. Wan, C. L. Bai, *Angew. Chem.* **2004**, *116*, 1566–1569; *Angew. Chem. Int. Ed.* **2004**, *43*, 1540–1543.

[8] a) B. Liu, H. C. Zeng, *Small* **2005**, *1*, 566–571; b) Y. Chang, J. J. Teo and H. C. Zeng, *Langmuir* **2005**, *21*, 1074–1079.

[9] K. M. Nam, J. H. Shim, H. Ki, S. Choi, G. Lee, J. K. Jang, Y. Jo, M. Jung, H. Song, J. T. Park, *Angew. Chem.* **2008**, *120*, 9646–9650; *Angew. Chem. Int. Ed.* **2008**, *47*, 9504–9508.

[10] Y. G. Sun, B. Mayers, Y. N. Xia, *Adv. Mater.* **2003**, *15*, 641–646.

[11] Y. G. Sun, Y. N. Xia, *Adv. Mater.* **2004**, *16*, 264–268.

[12] A. Cabot, ; V. F. Puntes, E. Shevchenko, Y. Yin, L. Balcells, M. A. Marcus, S. M. Hughes, A. P. Alivisatos, *J. Am. Chem. Soc.* **2007**, *129*, 10358–10360; V. F. Puntes, E. Shevchenko, Y. Yin, L. Balcells, M. A. Marcus, S. M. Hughes, A. P. Alivisatos, *J. Am. Chem. Soc.* **2007**, *129*, 10358–10360.

[13] a) Y. Yin, R. M. Rioux, C. K. Erdonmez, S. Hughes, G. A. Somorjai, A. P. Alivisatos, *Science* **2004**, *304*, 711–716; b) S. H. Kim, Y. D. Yin, A. P. Alivisatos, G. A. Somorjai, J. T. Yates, *J. Am. Chem. Soc.* **2007**, *129*, 9510–9513.

[14] a) J. Gao, G. Liang, B. Zhang, Y. Kuang, X. Zhang, B. Xu, *J. Am. Chem. Soc.* **2007**, *129*, 1428–1433; b) J. Lee, J. C. Park, H. Song, *Adv. Mater.* **2008**, *20*, 1523–1528.

[15] A. E. Henkes, Y. Vasquez, R. E. Schaak, *J. Am. Chem. Soc.* **2007**, *129*, 1896–1897.

[16] S. Peng, S. Sun, *Angew. Chem.* **2007**, *119*, 4233–4236; *Angew. Chem. Int. Ed.* **2007**, *46*, 4155–4158.

[17] J. Yang, H. I. Elim, Q. B. Zhang, J. Y. Lee, W. Ji, *J. Am. Chem. Soc.* **2006**, *128*, 11921–11926.

[18] J. Joo, H. B. Na, T. Yu, J. H. Yu, Y. W. Kim, F. Wu, J. Z. Zhang, T. Hyeon, *J. Am. Chem. Soc.* **2003**, *125*, 11100–11106.

[19] S. M. Lee, Y. W. Jun, S. N. Cho, J. Cheon, *J. Am. Chem. Soc.* **2002**, *124*, 11244–11245.

[20] Y. Yin, C. Erdonmez, S. Aloni, A. P. Alivisatos, *J. Am. Chem. Soc.* **2006**, *128*, 12671–12673.

[21] NIST X-ray Photoelectron Spectroscopy Database, Ver 3.5 online. http://srdata.nist.gov/gateway/gateway?keyword = XPS.

[22] A. Kumar, S. Mandal, P. R. Selvakannan, R. Pasricha, A. B. Mandale, M. Sastry, *Langmuir* **2003**, *19*, 6277–6282.

[23] L. Cademartiri, J. Bertolotti, R. Sapienza, D. S. Wiersma, G. von Freymann, G. A. Ozin, *J. Phys. Chem. B* **2006**, *110*, 671–673.

[24] a) J. Liu, H. Yu, Z. Wu, W. Wang, J. Peng, Y. Cao, *Nanotechnology* **2008**, *19*, 345602; b) M. S. Bakshi, P. Thakur, S. Sachar, G. Kaur, T. S. Banipal, F. Possmayer, N. O. Petersen, *J. Phys. Chem. C* **2007**, *111*, 18087–18098.

[25] a) M. J. Scaini, G. M. Bancroft, S. W. Knipe, *Geochim. Cosmochim. Acta* **1997**, *61*, 3565–3585; b) M. J. Scaini, G. M. Bancroft, J. W. Lorimer, L. M. Maddox, *Geochim. Cosmochim. Acta* **1995**, *59*, 2733–2747.

[26] a) C. M. Eggleston, M. F. Hochella, Jr., *Science* **1991**, *254*, 983–986; b) C. M. Eggleston, M. F. Hochella, Jr., *Am. Mineral.* **1993**, *78*, 877–883.

[27] A. Starling, J. M. Gilligan, A. H. C. Carter, R. P. Foster, R. A. Saunders, *Nature* **1989**, *340*, 298–300.

[28] J. R. Mycroft, G. M. Bancroft, N. S. McIntyre, J. W. Lorimer, *Geochim. Cosmochim. Acta* **1995**, 59, 3351–3365.

[29] L. Carbone, S. Kudera, C. Giannini, G. Ciccarella, R. Cingolani, P. D. Cozzoli, L. Manna, *J. Mater. Chem.* **2006**, *16*, 3952–3956.

[30] Y. Xiong, B. Wiley, J. Chen, Z. Y. Li, Y. D. Yin, Y. N. Xia, *Angew. Chem.* **2005**, *117*, 8127–8131; *Angew. Chem. Int. Ed.* **2005**, *44*, 7913–7917.

[31] C. C. Huang, J. R. Hwu, W. C. Su, D. B. Shieh, Y. H. Tzeng, C. S. Yeh, *Chem. Eur. J.* **2006**, *12*, 3805–3810.

[32] W. Shi, H. Zeng, Y. Sahoo, T. Y. Ohulchanskyy, Y. Ding, Z. L. Wang, M. Swihart, P. N. Prasad, *Nano Lett.* **2006**, *6*, 875–881.

[33] J. S. Lee, E. V. Shevchenko, D. V. Talapin, *J. Am. Chem. Soc.* **2008**, *130*, 9673–9675.